Desorption experiments and modeling of micropollutants on activated carbon in water phase: application to transient concentrations mitigation

Séda Bourneuf, Matthieu Jacob, Claire Albasi, Sabine Sochard, Romain Richard, Marie-Hélène Manero

Desorption experiments and modeling of micropollutants on activated carbon in water phase: application to transient concentrations mitigation

S. Bourneuf[1,2,3] · M. Jacob[3] · C. Albasi[2] · S. Sochard[4] · R. Richard[1,2] · M. H. Manero[1,2]

Abstract Experimental studies and numerical modeling were conducted to assess the feasibility of a granular activated carbon column to buffer load variations of contaminants before wastewater treatment devices. Studies of cycles of adsorption, and more especially desorption, of methyldiethanolamine (MDEA) and 2,4-dimethylphenol (2,4-DMP) have been carried out on granular activated carbon (GAC). Dynamic variations of contaminants concentrations were run at several conditions of duration (peaks). GAC fixed-bed exhibited a stable adsorption/desorption capacity after undergoing two conditioning cycles. The study of pollution peaks revealed that attenuation is largely dependent on the targeted pollutant: 2.4 ± 0.5 % attenuation/cm of bed for MDEA and 6.0 ± 1.2 % attenuation/cm of bed for 2,4-DMP. Mass balances calculated from both injected and recovered pollutant during peaks were respected. Finally, a coupling of the linear driving force model and isotherms models was used to fit experimental data for both adsorption breakthrough curves and desorption curves. The model was used to predict adsorption and desorption behaviors of following cycles. Good agreement with experimental values was obtained.

✉ S. Bourneuf
seda.bourneuf@gmail.com

[1] Laboratoire de Génie Chimique, INPT, UPS, Université de Toulouse, 4, Allée Emile Monso, 31030 Toulouse, France

[2] Laboratoire de Génie Chimique, CNRS, 31030 Toulouse, France

[3] TOTAL, PERL - Pôle d'Etudes et de Recherche de Lacq, RN 117, BP 47, 64170 Lacq, France

[4] Laboratoire de Thermique Energétique & Procédés, ENSGTI, Université Pau et Pays de l'Adour, Rue Jules Ferry, BP 7511, 64075 Pau Cedex, France

Keywords Adsorption · Desorption · Activated carbon · Water treatment · Modeling · LDF · Organics

Introduction

Applied context

Industrial activities generate a large variety of contaminated effluents which require an appropriate treatment before being released into the environment. Depending on the sector of activity, nature and constitution of the effluent, regulations in force, etc., various treatments are implemented. This is the case of wastewater devices such as biofilters or activated sludge. Due to the unsteady-state nature of industrial processes, variations of effluents charge with time (flow and/or concentrations) are very often encountered: daily variations in operating conditions, hourly fluctuations or even more frequent variations caused by process conditions and operations. Most of the time, they negatively impact running forthcoming treatments, with risks of leading to non-respect of discharge norms (Wani et al. 1998; Fitch et al. 2002; Kim et al. 2005; Alinsafi et al. 2006). In order to avoid this, buffering of wastewater treatment is generally achieved by equalization basins (Argaman et al. 2000). However, their setup exhibits major disadvantages (large areas, cost, maintenance (Tchobanoglous et al. 2002). In this context, an alternative solution could be to set up a column of adsorbent, prior to treatment as a buffer/equalizer unit.

At the phenomena scale

The reversibility of adsorption phenomena is one of its interesting features. Thanks to this property, the regeneration of spent adsorbents is usual, through different

kinds of techniques: hot water desorption (Berčič et al. 1996; Zhonghua Hu et al. 2000), solvent-assisted desorption (Kim and Kim 2004; Tanthapanichakoon et al. 2005; Muhammad et al. 2011), saline solution desorption (de Jonge et al. 1996; Ozkaya 2006) or by addition of a polymer (Johnson and Weber 2001). On an other hand, a few studies propose to use the versatility of adsorption to design a new kind of pre-treatment step before operations that are particularly sensitive to inlet variations of charge (Cox and Deshusses 2002; Iranpour et al. 2005). During periods of high loading, contaminants would accumulate into the adsorbent. When the inlet charge would return to a usual load, contaminants would progressively be released out of the adsorbent column. By means of this process, a buffering of dynamic load variations could be achieved and contamination loading would be distributed more consistently over time (Fig. 1). Previous studies on such buffering strategy have focused on treatment of gases (Weber and Hartmans 1995; Li and Moe 2005; Moe and Li 2005; Kim et al. 2007; Cai and Sorial 2009). Data for such treatments on wastewater lines are scarce, and very few experimental works or modeling was found on this subject.

Gaseous development

This strategy, first proposed by Ottengraf (1986), has been tested for gaseous effluents treatment (Weber and Hartmans 1995; Li and Moe 2005; Moe and Li 2005; Kim et al. 2007; Cai and Sorial 2009; Nabatilan and Moe 2010). These authors have proven the efficiency of a column of adsorbent to buffer gaseous load variations of volatile organic compounds such as toluene, acetone, styrene, methyl ethyl ketone or methyl isobutyl ketone, and found out significant improvement in following air biofilters efficiency. In all these reports, the adsorption of a pure component (toluene) on granular activated carbon was studied as the first step to determine the ranges of loads that can be buffered as a function of the studied conditions (Weber and Hartmans 1995; Moe and Li 2005; Kim et al. 2007). These first investigations generally proposed to use a model calibration to fit experimental data and predict future device setup. The chosen models were linear driving force (LDF) (Kim et al. 2007) or pore and surface diffusion model (PSDM) (Moe and Li 2005). A further step of these studies essentially consisted of experimental trials with multi-components gaseous mixtures (Li and Moe 2005; Cai and Sorial 2009). PSDM model was successfully used to fit data for an acetone/toluene mixture (Li and Moe 2005), pointing out the competitive behavior of components dealing with expected buffering effect. Good fitting between experimental data and PSDM (Crittenden et al. 1980; Hand et al. 1997) enabled the prediction of the load-buffering achieved by granular activated carbon (GAC) columns under discontinuous loading conditions.

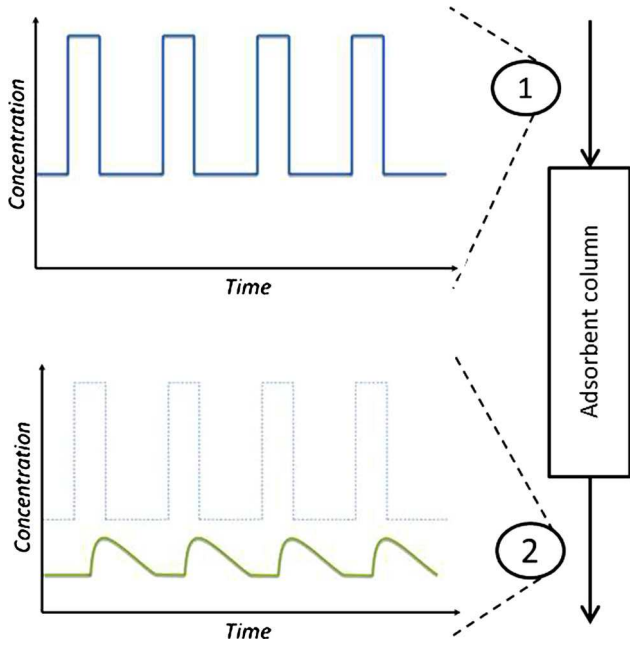

Fig. 1 Theoretical buffering strategy using an adsorbent column to prevent from load variations

In the present study

The objective of this study is to conduct experiments while performing numerical simulation to assess the feasibility of activated carbon column to play this buffer role in an industrial context of petroleum wastewater treatment. In this case, major contaminants are hydrocarbons (BTEX, PAHs), chlorinated solvents and phenolic derivatives (Leglize et al. 2006). Very few researches have been reported on desorption of a fixed-bed column caused by the variation of contaminant loading *in water phase*.

This work aims to assess the ability of a column of adsorbent to buffer aqueous phase load variations through cycles of adsorption and desorption when facing pollution peaks. It was carried out on laboratory-scale columns of granular activated carbon, through conventional steps for adsorption studies, that is to say adsorption isotherms determination, followed by adsorption/desorption cycles to appreciate the load attenuation. Besides, modeling of both experimental adsorption and desorption curves was accomplished with the combination of linear driving force and isotherm models. The research has been carried out in the Chemical Engineering Laboratory, Toulouse, France (2014).

Materials and methods

Chemicals and adsorbent

Two contaminants widely found in various wastewaters such as cosmetic, pharmaceutical or petroleum industries have been selected: 2,4-dimethylphenol (2,4-DMP) and methyldiethanolamine (MDEA). These contaminants have been chosen as they are of general concern but also because of their facility of manipulation and quantification. Moreover, another interest resides in their different properties which presuppose various behaviors during adsorption and desorption.

MDEA (≥99 %) and 2,4-DMP (98 %) were purchased from Sigma-Aldrich, and aqueous solutions were prepared in demineralized water. Their main physicochemical properties consist of molecular weights of 119.2 and 122.2 g/mol and $\log K_{ow}$ value of −1.08 and 2.35 for MDEA and 2,4-DMP, respectively.

Granular activated carbon (GAC 1240) was provided by Ceca (France). This mineral micro/mesoporous activated carbon has a BET surface of 892 m^2/g, a pore volume of 0.47 mL/g and an average particle diameter of 1 mm. Prior to experimentation, the materials were washed with ultrapure water, drained, dried at 105 °C for 24 h and then kept in a hermetic vial before use.

Experimental setup

Batch experiments

The adsorption isotherms were determined using various amounts of adsorbent (between 0.05 and 2 g) in glass bottles with 250 mL of a feedstock solution. The bottles were sealed and stirred during 48 h using a thermoregulated bath at 25 ± 1 °C.

Fixed-bed experiments

Continuous adsorption/desorption runs were conducted on an experimental setup consisting of small glass columns with an internal diameter of 15 mm. Columns were loaded with various masses of activated carbon in order to operate with a reasonable experience duration (total breakthrough within 10 h): 5 g for 2,4-DMP and 10 g for MDEA experiments. Total GAC packed bed depth was 12.0 and 6.5 cm for MDEA and 2,4-DMP experiments, respectively. Prior to experimentation, columns were rinsed with distilled water for 2 h and air bubbles were removed with the help of a stirrer. Columns were fed with stock solutions of MDEA or 2,4-DMP at a concentration C_0 of 2 g/L thanks to a Minipulse Gilson peristaltic pump at a flowrate of 4.0 ± 0.2 mL/min (empty bed contact time (EBCT) = 5.5 and 3.0 min for MDEA and 2,4-DMP, respectively). Solution samples were collected at the output of the columns, diluted and analyzed. Experiments were carried out at a temperature of 22 ± 2 °C.

Experimental cycles of adsorption and desorption were run with columns successively fed with C_0 stock solutions during the adsorption step and deionized water during the desorption step. The experiments were stopped when no variations in exiting solutions occurred, showing that equilibrium is reached.

Pollution peaks were also studied on a pre-equilibrated column (after an adsorption breakthrough). Once the value of C/C_0 was stabilized, peaks were created by switching the feeding solution at concentration C by another solution at concentration $C \times 2$ during 20 min. Then, the alimentation was switched again to go back to concentration C. As for cycle experiments, runs were conducted until no variation of concentration was observed in samples of solution samples collected at the columns outputs.

Analytical method

Batch experiment samples were collected from each bottle and filtered through 0.45-μm nylon filters, and the residual aqueous concentration in MDEA or 2,4-DMP was determined by total carbon (TC) analysis, after dilution when necessary to match the analytical range. For fixed-bed experiments, samples were collected at column outlets and aqueous concentration in MDEA or 2,4-DMP was also determined by TC analysis, after dilution when necessary to match the analytical range.

The total carbon (TC) was determined using a Shimadzu TOC-V series with a precision of 2 %. Analysis was performed using an infrared cell and two calibration curves (0–50 and 0–100 mg/L).

Modeling strategy

The mathematical model of the isothermal, dynamic adsorption breakthrough process in a fixed bed is based on transient material balance, liquid phase (external) mass transfer, intrapellet mass transfer, adsorption equilibrium relationship, boundary conditions and initial conditions. Both adsorption equilibrium and kinetics aspect are taken into account. The mass-transfer rate is represented by the LDF model (Glueckauf 1955). The LDF model is a lumped-parameter model for particle adsorption. If the flow rate is assumed constant, the mass balance on a portion of the bed is given by Eq. (1) (Ruthven 1984; Tien 1995).

$$\frac{\partial C}{\partial t} = -u\frac{\partial C}{\partial z} + D_{ax}\frac{\partial^2 C}{\partial z^2} - \rho_{AC}\frac{1-\varepsilon}{\varepsilon}\frac{\partial \bar{q}}{\partial t} \quad (1)$$

where C is the concentration in the liquid phase (mol/m^3), D_{ax} the axial dispersion coefficient (m^2/s), u the superficial rate (m/s), ε the bed porosity, ρ_{AC} the activated carbon density (kg/m^3) and $\bar{q}$ the average amount adsorbed (mol/kg).

In this study, the LDF model was used to describe the intrapellet mass transfer (Brosillon et al. 2001):

$$\frac{\partial \bar{q}}{\partial t} = k_p(q_s - \bar{q}) \tag{2}$$

and

$$k_C S_p(C - C_s) = \rho_{AC}(1 - \varepsilon)k_p(q_s - \bar{q}) \tag{3}$$

where the lumped parameter k_p (s^{-1}) includes the intrapellet mass-transfer coefficient and eventually surface diffusion if present, k_c is the bulk mass-transfer coefficient (m/s), S_p the specific surface of the bed (m^2/m^3) (for spherical particles of diameter d_p, S_p is equal to $6(1 - \varepsilon)/d_p$) and C the concentration in liquid phase (mol/m^3).

C_s (mol/m^3) and q_s (mol/kg) are, respectively, the concentration in the liquid and the amount adsorbed at the surface, at the interface between the liquid phase and the adsorbent. Since equilibrium is assumed at this interface, C_s and q_s are linked by the isotherm equilibrium. Adsorption equilibrium can be described by Langmuir (1916) or Freundlich (1906) equations. The choice of the model of the isotherm equilibrium is discussed later.

k_c is estimated by the semi-empirical equation of Wakao and Funazkri (1978):

$$Sh = 2 + 1.1\, Re^{0.6} Sc^{0.3} \tag{4}$$

and

$$Sh = \frac{k_C d_p}{D_{ax}} \tag{5}$$

Sh, Re and Sc are the dimensionless numbers of Sherwood, Reynolds and Schmidt.

D_{ax} is estimated by the following correlation (Delgado 2007).

$$D_{ax} = \frac{u d_P}{\varepsilon \sqrt{18\left(\tau \frac{Re\, Sc}{\varepsilon}\right)^{-1.2} + 2.35\, Sc^{-0.38}}} \tag{6}$$

τ is the tortuosity factor which is assumed to be equal to 4 in the present study, value usually encountered for AC's columns (Perry and Chilton 1973; Ruthven 1984).

The model is solved by discretizing the space value z. The resulting algebro-differential system is then solved using the ode15s function in Matlab®. The initial profiles of the liquid concentration and of the adsorbed amount in the column, at the beginning of an adsorption or desorption stage, are those obtained at the end of the previous stage, except for the first adsorption stage where all the values are set to 0.

It is possible to carry out identification of the k_p parameter. This identification can be done on a single adsorption or desorption breakthrough, an adsorption–desorption cycle or even several adsorption–desorption cycles. The identification is carried out by minimizing the following criterion, which is defined by the sum of the relative squared differences between the experimental measured data and the model output at different reaction times:

$$\text{Minimization criterion} = \frac{1}{n_{exp}} \sum_i \left(\frac{C_{OUT}(i)_{mod} - C_{OUT}(i)_{exp}}{C_{OUT}(i)_{exp}} \right)^2 \tag{7}$$

where $C_{OUT}(i)_{mod}$ is the calculated concentration at the outlet of the column at reaction time i, $C_{OUT}(i)_{exp}$ is the experimental concentration at the outlet of the column at reaction time $i = 1, 3$ min,… several hours, and n_{exp} is the number of experimental concentrations.

The criterion chosen is the sum of squared relative errors (SSRE) instead of the classical sum of squared (absolute) errors (SSE). Indeed, some concentrations such as concentrations at the end of desorption cycles are much lower than the concentrations at the end of adsorption cycle for example, so that differences in concentrations at the end of desorption cycles would be ineffective with SSE criterion but would generate very important variations with SSRE criterion by comparison with errors at the end of adsorption cycles. Thus, working with a criterion on relative variations, errors at any time are balanced, which is more representative of the system.

Results and discussion

Adsorption isotherms

The results of the adsorption isotherms carried out for the two selected compounds (2,4-DMP and MDEA) are presented in Fig. 2. The amount of adsorbed pollutant increases with the equilibrium concentration: Isotherms are favorable and can be described in the range of concentrations tested as type II according to the IUPAC classification (Sing 1985). This category of reversible isotherms is a characteristic of most activated carbons, adsorbents with a large distribution of pores. Other kinds of isotherms were found with 2,4-DMP on microporous crystalline adsorbents (Aboussaoud et al. 2014) showing unrestricted monolayer–multiplayer adsorption.

The adsorption capacity of the selected activated carbon is more important for 2,4-DMP than for MDEA. Indeed, whatever the equilibrium concentration in the aqueous phase, results indicate that the value of q_e is consistently higher for 2,4-DMP than for MDEA. Generally, activated

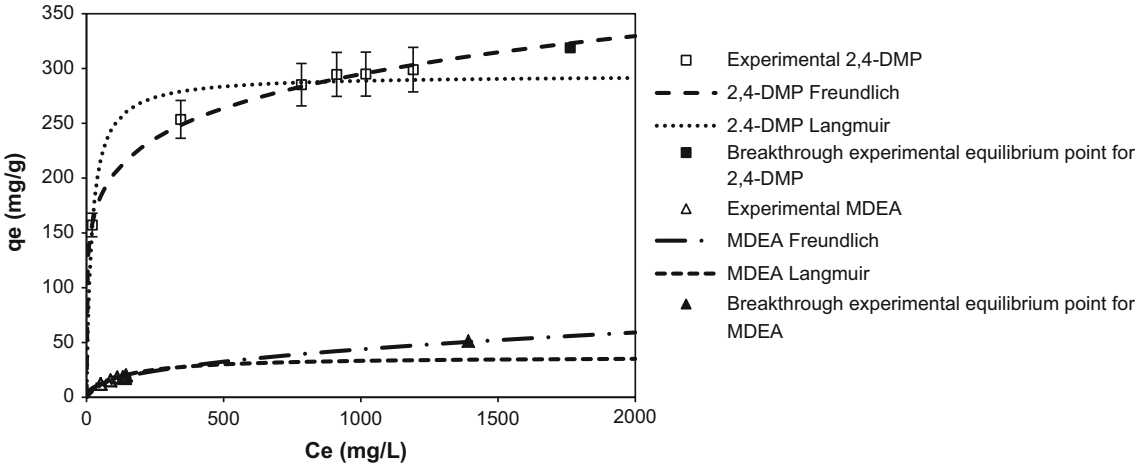

Fig. 2 Batch experimental and modeled adsorption isotherms for 2,4-DMP and MDEA ($T = 25$ °C)

Table 1 Freundlich and Langmuir isotherms parameters for MDEA and 2,4-DMP

Pollutant	Freundlich			Langmuir		
	$1/n$	K	R^2	b	q_m (mg/g)	R^2
MDEA	0.44	2.2	0.991	0.01	37.2	0.902
2,4-DMP	0.16	96.5	0.997	0.05	294.1	0.978

carbons preferentially adsorb nonpolar or weakly polar components (Crittenden and Thomas 1998). The polarity of a molecule is tightly related to its partition coefficient K_{ow}. The characteristics of adsorbates, given in part 2.1., indicates that log $K_{ow} = -1.08$ and 2.35 for MDEA and 2,4-DMP, respectively. Thus, the hydrophobicity of 2,4-DMP, mostly because of the presence of an aromatic cycle, is higher than of MDEA. For this reason, 2,4-DMP is logically more adsorbed on activated carbon.

Freundlich and Langmuir Eqs. (8, 9), which are the most frequently employed in liquid/solid adsorption studies, were selected to model the adsorption behavior of MDEA and 2,4-DMP:

$$q_e = K.C_e^{1/n} \tag{8}$$

$$q_e = \frac{b.q_m.C_e}{1 + b.C_e}. \tag{9}$$

where q_e is the amount adsorbed at equilibrium (mg/g), C_e is the equilibrium liquid phase concentration (mg/L), K and n are Freundlich fitting parameters, q_m is the maximum amount adsorbed (mg/g) and b is the Langmuir constant. Freundlich and Langmuir parameters can be, respectively, determined through linearization. Results are presented in Table 1.

Freundlich model appears to be the most suitable to describe our experimental data with $R^2 \geq 0.991$, while the regression coefficients R^2 obtained with Langmuir model does not exceed 0.978. It is interesting to compare the K values obtained for each compound: $K_{MDEA} = 2.2$ and $K_{2,4\text{-DMP}} = 96.5$. As a larger K value represents a larger adsorption capacity, these values correspond with our previous comments and clearly prove a greater affinity of 2,4-DMP for GAC1240. This result is in agreement with observations made by Mason et al. (2000): AC's adsorption capacity is inversely related to compound's solubility. Previous studies performed on the adsorption of 2,4-DMP and MDEA on activated carbon confirmed best fitting with Freundlich model. Lesage (2005) obtained 0.31 for $1/n$ and 50.0 for K for the adsorption of 2,4-DMP on organic AC (BET surface = 1707 m^2/g and porous volume = 0.745 mL/g) whereas Chakma and Meisen (1989) found 0.26 and 47.7 for $1/n$ and K, respectively, for the adsorption of MDEA on mineral SGL AC (specific surface area between 950 and 1050 m^2/g, pore volume = 0.85 mL/g). Moreover, values obtained in this work are in the same range as values obtained previously with other activated carbons. The better performances, observed by Chakma and Meisen (1989), can probably find explanations in AC characteristics as the SGL pore volume is higher than the value determined for GAC 1240 used in this study (0.47 mL/g). Concerning the differences in adsorption capacity obtained by Lesage (2005), they may be attributed to other AC specifications such as its origin. Indeed, previous works verified that mineral ACs exhibit higher adsorption capacity for organic compounds than organic ACs (Snoeyink et al. 1969; Choi et al. 2005).

Fixed-bed GAC adsorption/desorption tests

Several cycles of adsorption/desorption experiments were conducted on a fixed bed of activated carbon using a continuous single component loading of 2,4-DMP or MDEA to assess the reversibility of adsorption on GAC 1240 and the repeatability of a single adsorption/desorption

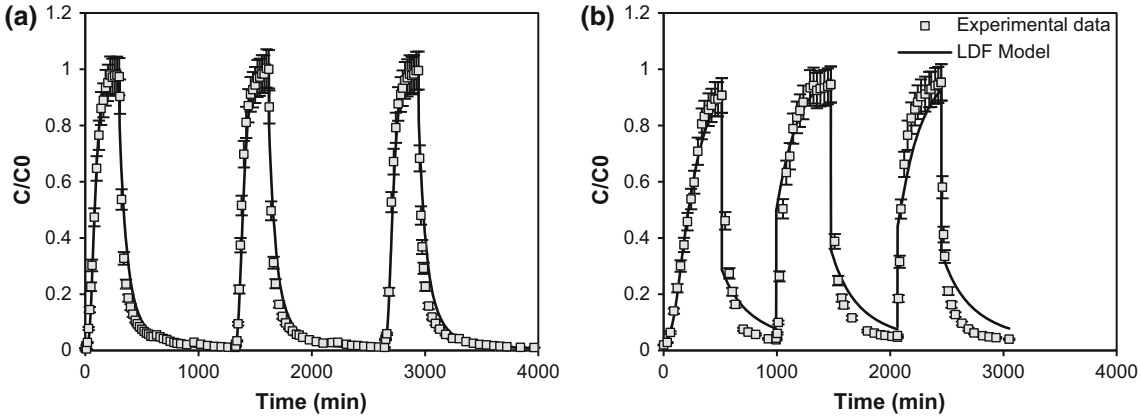

Fig. 3 Experimental values and modeled cycles of adsorption and desorption for **a** MDEA (21 ± 1 °C) and **b** 2,4-DMP (22 ± 1 °C) on a fixed bed of activated carbon

experiment. Figure 3 presents the results obtained for MDEA (a) and 2,4-DMP (b). For both compounds, it is possible to repeat cycles of adsorption/desorption and their desorbability is confirmed. The amounts adsorbed on virgin carbon during the first cycle (318.9 mg/g for 2,4-DMP and 50.0 mg/g for MDEA) are very close to the amounts predicted by the Freundlich model: 330.6 and 48.3 mg/g for 2,4-DMP and MDEA, respectively, which represents a difference of 3.5 %. It can be noticed that Freundlich model is less accurate to predict the amount of contaminant adsorbed during the following cycles. For those cycles, prediction of adsorption capacity would require the achievement of adsorption isotherm on used GAC (AC with its sites of irreversible adsorption pre-saturated) or would have to be deduced from percentages of irreversibility by taking into account the AC state at the end of the first cycle.

The LDF model was calibrated using experimental data for the first cycle of adsorption and desorption. The values of k_c and D_{ax} used for each compound are presented in Table 2. Simulation results presented in Fig. 3 were obtained with the value of the lumped parameter k_p identified during the first cycle of adsorption and desorption. Identifications performed on the other cycles led to slightly the same values. Best agreement between experimental data and modeled data is achieved for adsorption breakthrough during the first cycle. Indeed, adsorption minimization criterions (<0.06) are better than those obtained for desorption (>3), which reveals that desorption stages are less well represented by the LDF model, and a phenomenon which is not taken into account in this model should be considered in further work to obtain perfect fitting of model with experimental data.

Otherwise, LDF model gives better correlation of experimental data on the first cycle for each contaminant. In fact, since the LDF model is less efficient to well represent the desorption stage, the initial profiles of the liquid concentration and of the adsorbed amount in the column at the beginning of the adsorption stage of cycles 2 and 3 were less precise. The adsorption profile during cycles 2 and 3 is well represented even if the fitting is not as accurate as for the first adsorption stage. Globally, minimization criterion values obtained for MDEA and 2,4-DMP are not significantly different from one compound to the other. By visual observations, it seems that LDF model provides better fitting for MDEA than for 2,4-DMP, but no clear conclusion can be made on this comparison. However, identified k_p values can be compared. The values obtained indicate a higher diffusion for MDEA than for 2,4-DMP. This difference can be explained by the molecule structures. Indeed, with its aromatic cycle, 2,4-DMP has a larger molecule diameter than MDEA which induces steric interferences with activated carbon pores.

Table 2 Parameters used for LDF modeling of MDEA and 2,4-DMP cycles of adsorption and desorption and minimization criterions obtained for fist adsorption and desorption step

Parameter	MDEA	2,4-DMP
k_c (m/s)	5.9×10^{-6}	7.1×10^{-6}
D_{ax} (m^2/s)	4.2×10^{-6}	4.0×10^{-6}
k_p (s^{-1})	6.4×10^{-4}	1.2×10^{-4}
Adsorption minimization criterion	0.054	0.032
Desorption minimization criterion	6.70	3.65

Breakthrough curves for MDEA and 2,4-DMP obtained during cycles of adsorption and desorption (Fig. 3) have been gathered and are depicted in Fig. 4a, b for adsorption curves and Fig. 4c, d for desorption curves. For both compounds, the first breakthrough curve exhibits a specific shape, whereas breakthrough curves obtained during cycle 2 and 3 are almost undistinguishable, in particular for MDEA. This suggests differences in the adsorption of

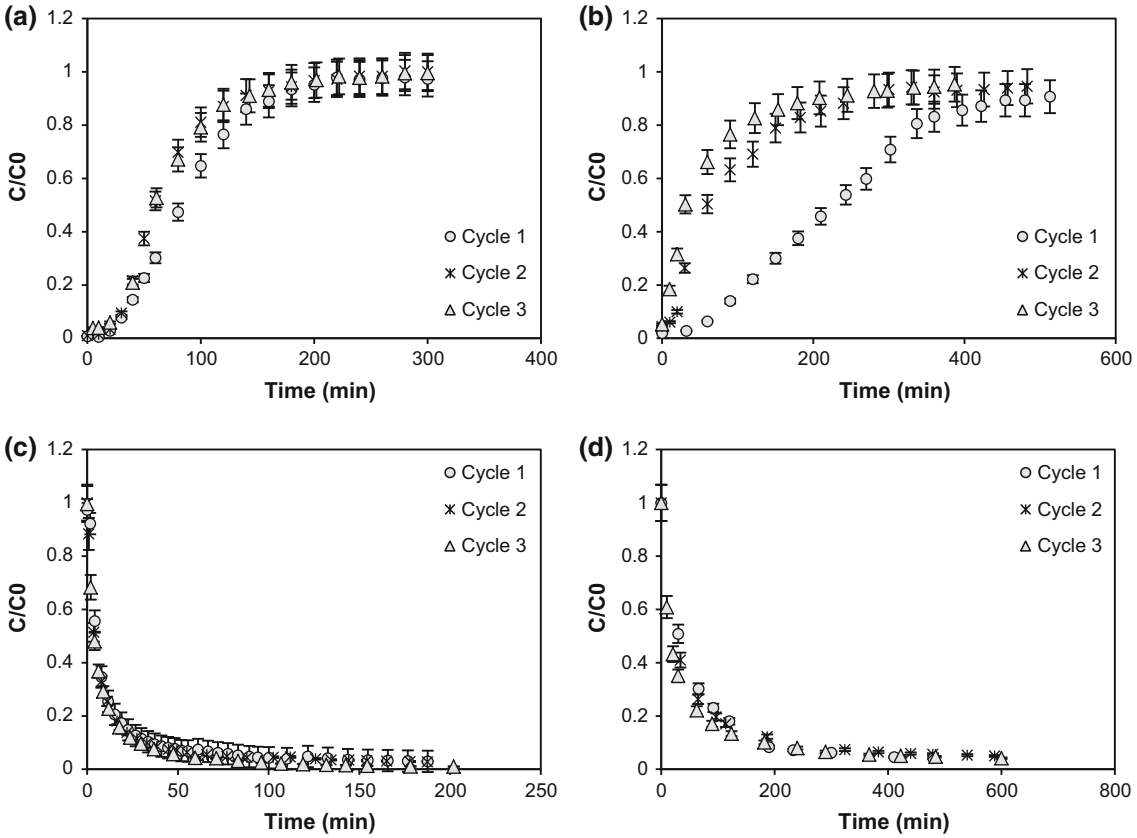

Fig. 4 Breakthrough curves for **a** MDEA (21 ± 1 °C) and **b** 2,4-DMP (22 ± 1 °C) adsorption and desorption curves for **c** MDEA (21 ± 1 °C) and **d** 2,4-DMP (22 ± 1 °C) during cycles on fixed-bed column of activated carbon (GAC 1240)

pollutant depending on whether the cycle is the first one and hence the state of the activated carbon, whereas no clear distinction has been observed for desorption curves (Fig. 4c, d). Whatever the compound (MDEA or 2,4-DMP), the three desorption curves can be overlaid. It can therefore be concluded that the state of the activated carbon (virgin for cycle 1 or re-used for cycles 2 and 3) does not impact desorption profiles.

Amounts of 2,4-DMP and MDEA adsorbed and desorbed through the three cycles are gathered in Table 3. The mass of pollutant desorbed during the first cycle is less important than the quantity previously adsorbed. This result indicates that adsorbed pollutant cannot be totally desorbed because of a partial irreversibility of the adsorption process. This trend has already been reported in previous work on activated carbon (Moe and Li 2005) or on other materials such as zeolites (Merle 2009). This phenomenon probably results from differences in the strength of contaminant adsorption on high-energy and low-energy sites. During the first breakthrough experiment, pollutant molecules can be adsorbed on any adsorption sites, but during the desorption step, only molecules adsorbed on low-energy adsorption sites are able to be released.

Table 3 Amounts adsorbed and desorbed, capacities of adsorption and percentages desorbed after 8 h and totally desorbed for 2,4-DMP and MDEA during cycles 1, 2 and 3

Cycle	m_{ads} (mg)	m_{des} (mg)	q (mg/g)	Total % desorbed
MDEA				
1	500 ± 51	380 ± 39	50 ± 5	76 ± 16
2	430 ± 44	405 ± 41	43 ± 4	94 ± 19
3	373 ± 38	406 ± 41	37 ± 4	109 ± 22
2,4-DMP				
1	1648 ± 168	473 ± 32	319 ± 33	29 ± 5
2	638 ± 65	471 ± 32	124 ± 13	74 ± 13
3	366 ± 26	322 ± 22	71 ± 5	88 ± 12

Throughout the following cycles, the proportion of available high-energy adsorption sites is reduced because part of them is already occupied, and thus the proportion of irreversibility is reduced. Indeed, the total percentage of desorbed pollutant increases from 29 to 88 % for 2,4-DMP over cycles. For MDEA, the irreversibility of adsorption is less pronounced with a desorption ratio of 76 % during first cycle and 109 % for the last one. As MDEA is less hydrophobic than 2,4-DMP, its adsorption is more

Table 4 Initial adsorption and desorption rates of MDEA and 2,4-DMP during cycles

Cycle	MDEA				DMP			
	Adsorption		Desorption		Adsorption		Desorption	
	$r_{initial}$ (mg L/min)	R^2	$r_{initial}$ (mg L/min)	R^2	$r_{initial}$ (mg L/min)	R^2	$r_{initial}$ (mg L/min)	R^2
1	4.8 ± 0.8	0.883	−17.8 ± 3.1	0.981	3.0 ± 0.5	0.981	−10.3 ± 1.8	0.966
2	7.4 ± 1.3	0.982	−18.9 ± 3.2	0.975	12.5 ± 2.1	0.933	−9.5 ± 1.6	0.941
3	6.1 ± 1.0	0.941	−19.3 ± 3.3	0.990	13.9 ± 2.4	0.759	−13.9 ± 2.4	0.903

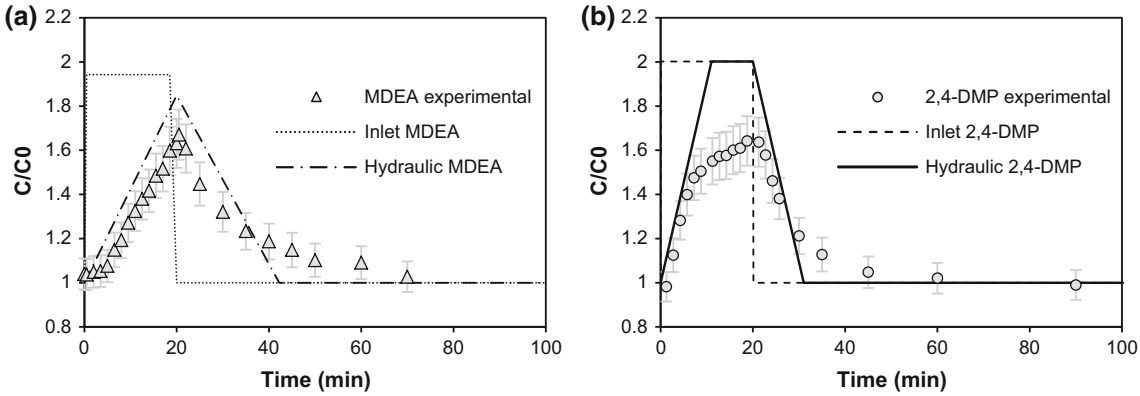

Fig. 5 Single component peaks of **a** MDEA and **b** 2,4-DMP on fixed-bed AC column. Experimental conditions: inlet concentration multiplied by 2 during 20 min

reversible than 2,4-DMP adsorption. Thus, cycle curve shapes depend on the ability of the contaminant to be adsorbed and desorbed.

Kinetics of adsorption and desorption have also been investigated. Initial adsorption and desorption rates are presented in Table 4. For both contaminants, the initial rate of the first adsorption is lower than the ones observed in the next cycles. Complete breakthrough (considered for $C/C_0 > 0.95$) was obtained after 180 min for MDEA whatever the cycle. For 2,4-DMP, time required to reach this point was more important: up to 500 min for the first cycle and more than 400 min for cycles 2 and 3. Taking into account that the bed used for MDEA experiments is twice higher than the one used for 2,4-DMP experiments, this difference is even more important and reveals once again, a higher adsorption capacity of 2,4-DMP than that of MDEA on GAC1240. Concerning desorption, the initial rate for MDEA is almost three times higher than the initial adsorption rate. The behavior is different for 2,4-DMP: except the first adsorption rate, initial desorption rates are almost equivalent to those of adsorption. On desorption experiments, a value of $C/C_0 < 0.05$ was reached after 60 min for MDEA versus 400 min for 2,4-DMP.

Gradually, the quantities of contaminant adsorbed and desorbed tend toward equilibrium by stabilization of the GAC column adsorption/desorption capacity.

Load attenuation by GAC columns

Experimentally measured concentrations exiting a fixed-bed column of activated carbon undergoing a single component peak of pollution are presented in Fig. 5. Breakthrough equilibrium was previously reached on two separated columns (one for MDEA and the other for 2,4-DMP) and then used several times before peaks were conducted on each of them. The results obtained indicate a capacity of the AC column to attenuate various concentration loads: maximum C/C_0 values reached for MDEA and 2,4-DMP were, respectively, 1.67 and 1.64, whereas the inlet concentration was multiplied by two. Using Eq. (10), a percentage of attenuation can be estimated from experimental results:

$$\text{Attenuation } (\%) = \frac{(C_p - C_0) - (C_{max} - C_0)}{(C_p - C_0)} = \frac{(C_p - C_{max})}{(C_p - C_0)} \quad (10)$$

where C_p is the concentration of the peak entering the AC column (mg/L), C_0 is the initial inlet concentration (mg/L) and C_{max} is the maximal concentration reached at the end of the column (mg/L). Load attenuation percentages obtained are 29 ± 4 % for MDEA and 36 ± 5 % for 2,4-DMP. The AC column induces a reduction of one-third of

Table 5 Amounts of MDEA and 2,4-DMP injected into the AC column and recovered at the outlet during a peak of 20 min with a concentration multiplied by two

	MDEA	DMP
Injected mass (mg)	101.0 ± 6.9	130.0 ± 8.8
Recovered mass (mg)	94.6 ± 9.7	122.8 ± 12.6
% of disparity	6 ± 1 %	5 ± 1 %

the peak amplitude. Besides, load attenuation for MDEA and 2,4-DMP is not significantly different from each other. However, since the height of the fixed bed is different for each compound, this parameter should be taken into account in the calculation of the percentage of attenuation. For this reason, we propose to divide the attenuation coefficient by the height of the AC column. Values obtained are 2.4 ± 0.5 (MDEA) and 6.0 ± 1.2 (2,4-DMP) percent of load attenuation per centimeter of bed. Results are significantly different and the load attenuation coefficient of 2,4-DMP is about three times more important than the one calculated for MDEA. This is concordant with the previous observations: Activated carbon adsorption capacity increases with the hydrophobicity of the contaminant. A larger adsorption capacity may result in a higher ability to attenuate a pollution peak. Finally, hydraulic curves have been plotted: They represent a simple flow through a column without adsorption. Hydraulic curves are determined through EBCTs corrected with a tortuosity factor of 4 (Perry and Chilton 1973; Ruthven 1984). These curves demonstrate the buffering role of AC column since they indicate different profiles of attenuation which occur when no adsorption takes place in the fixed bed.

In order to assess whether accumulation of contaminant in the AC column occurs during pollution peaks or not, it is possible to compare amounts injected in the column to those recovered at the end of the column (Table 5). The quantity injected can easily be calculated knowing the inlet peak concentration, the flowrate and the peak duration. The amount of pollutant recovered is determined by graphical integration of the peak.

Amounts of pollutant injected in AC columns are entirely recovered (within 6 %) at the end of the column. Thus, it is possible to say that no permanent accumulation occurred in the bed of adsorbent during peaks after steady state was reached. Other authors such as Li and Moe (2005) observed the same phenomenon while treating load variations of toluene and acetone with a fixed bed of GAC. They also noticed various load attenuation capacities of activated carbon according to the targeted contaminant: Indeed attenuation was more pronounced for toluene than for acetone. It has been demonstrated that fixed bed of activated carbon acts like a buffer and could be used to treat multiple pollution peaks without loss of adsorption capacity since no contaminant seems to accumulate.

Conclusion

This work investigated the feasibility of activated carbon column to mitigate transient concentrations. The study of adsorption equilibria of 2,4-DMP and MDEA on GAC 1240 and its modeling by LDF and Freundlich isotherm models allowed the prediction of the component amount that can be adsorbed on virgin carbon during fixed-bed adsorption/desorption experiments. The two compounds showed some discrepancies in their behaviors, logically dependent on the chemical structure of the pollutant, the affinity decreasing with hydrophobicity and the presence of aromatic cycle.

Experimental work demonstrated the relatively good reversibility of adsorption phenomena on GAC 1240. Several cycles of adsorption and desorption could be successively run on a column of fixed-bed adsorbent. However, some irreversible phenomena were evidenced as a portion of pollutant was not desorbed during the first cycle. Desorption curves were reproducible from the second cycle. Concerning adsorption, the reproducibility was achieved after three cycles for both contaminants. After these three cycles, the GAC fixed bed exhibited a steady adsorption/desorption capacity.

Experiments carried out to simulate pollution peaks assessed that amounts of contaminants injected were recovered at the columns outlet. Contaminants (2,4-DMP and MDEA) temporarily accumulated in GAC columns during periods of high loading concentrations and were desorbed when influent concentrations were coming back to initial level. Thus, columns of adsorbent acted as a load buffer and were able to reduce the variations of charges. The percentage of attenuation achieved by the GAC column depended on the physicochemical properties of the pollutant.

The LDF model calibrated by optimizing the lumped parameter k_p showed very good fitting with experimental data for the first adsorption and gave reliable predictions for further cycles of adsorption and desorption.

Finally, results from this work showed that transient concentrations mitigation could be achieved by GAC columns. Complementary experiments should be run for a complete process setup, but these results are promising for a further implementation of an adsorbent column as a dampener in industrial wastewater treatment plants.

Acknowledgments The authors gratefully acknowledge the financial support for the research by French National Agency for Research and Technology and Total Group (CIFRE 2011/0925). The authors thank Dr. Nicolas Lesage for his support and helpful advices.

References

Aboussaoud W, Manero M-H, Pic J-S, Debellefontaine H (2014) Combined ozonation using alumino-silica materials for the removal of 2,4-dimethylphenol from water. Ozone Sci Eng 36:221–228

Alinsafi A, da Motta M, Le Bonté S et al (2006) Effect of variability on the treatment of textile dyeing wastewater by activated sludge. Dyes Pigments 69:31–39

Argaman Y, Raize O Jr, Eckenfelder W, O'Reilly AJ (2000) Applicability of batch test data for industrial wastewater continuous flow process design. Water Environ Res 72:348–352

Berčič G, Pintar A, Levec J (1996) Desorption of phenol from activated carbon by hot water regeneration. Desorption isotherms. Ind Eng Chem Res 35:4619–4625

Brosillon S, Manero MH, Foussard JN (2001) Mass transfer in VOC adsorption on zeolite: experimental and theoretical breakthrough curves. Environ Sci Technol 35:3571–3575

Cai Z, Sorial GA (2009) Treatment of dynamic VOC mixture in a trickling-bed air biofilter integrated with cyclic adsorption/desorption beds. Chem Eng J 151:105–112

Chakma A, Meisen A (1989) Activated carbon adsorption of diethanolamine, methyl diethanolamine and their degradation products. Carbon 27:573–584

Choi KJ, Kim SG, Kim CW, Kim SH (2005) Effects of activated carbon types and service life on removal of endocrine disrupting chemicals: amitrol, nonylphenol, and bisphenol-A. Chemosphere 58:1535–1545

Cox HHJ, Deshusses MA (2002) Effect of starvation on the performance and re-acclimation of biotrickling filters for air pollution control. Environ Sci Technol 36:3069–3073. doi:10.1021/es015693d

Crittenden B, Thomas WJ (1998) Adsorption technology & design. Butterworth-Heinemann, Boston

Crittenden JC, Wong BWC, Thacker WE et al (1980) Mathematical model of sequential loading in fixed-bed adsorbers. J Water Pollut Control Fed 52:2780–2795

De Jonge RJ, Breure AM, van Andel JG (1996) Reversibility of adsorption of aromatic compounds onto powdered activated carbon (PAC). Water Res 30:883–892

Delgado JMPQ (2007) Longitudinal and transverse dispersion in porous media. Chem Eng Res Des 85:1245–1252

Fitch MW, England E, Zhang B (2002) 1-Butanol removal from a contaminated airstream under continuous and diurnal loading conditions. J Air Waste Manag Assoc 52:1288–1297

Freundlich H (1906) Über die Adsorption in Lösungen. Wilhelm Engelmann, Leipzig

Glueckauf E (1955) Theory of chromatography. Part 10—Formulæ for diffusion into spheres and their application to chromatography. Trans Faraday Soc 51:1540–1551

Hand DW, Crittenden JC, Hokanson DR, Bulloch JL (1997) Predicting the performance of fixed-bed granular activated carbon adsorbers. Water Sci Technol 35:235–241

Hu Z, Srinivasan MP, Ni Y (2000) Adsorption and desorption of phenols and dyes on microporous and mesoporous activated carbons Adsorption science and technology. World Scientific, Singapore, pp 274–278

Iranpour R, Cox HHJ, Deshusses MA, Schroeder ED (2005) Literature review of air pollution control biofilters and biotrickling filters for odor and volatile organic compound removal. Environ Prog 24:254–267. doi:10.1002/ep.10077

Johnson MD, Weber WJ (2001) Rapid prediction of long-term rates of contaminant desorption from soils and sediments. Environ Sci Technol 35:427–433. doi:10.1021/es001392c

Kim S, Kim Y-K (2004) Apparent desorption kinetics of phenol in organic solvents from spent activated carbon saturated with phenol. Chem Eng J 98:237–243

Kim D, Cai Z, Sorial GA (2005) Evaluation of trickle-bed air biofilter performance under periodic stressed operating conditions as a function of styrene loading. J Air Waste Manag Assoc 55:200–209

Kim D, Cai Z, Sorial GA et al (2007) Integrated treatment scheme of a biofilter preceded by a two-bed cyclic adsorption unit treating dynamic toluene loading. Chem Eng J 130:45–52

Langmuir I (1916) The constitution and fundamental properties of solids and liquids. Part I. Solids. J Am Chem Soc 38:2221–2295

Leglize P, Saada A, Berthelin J, Leyval C (2006) Evaluation of matrices for the sorption and biodegradation of phenanthrene. Water Res 40:2397–2404

Lesage N (2005) Etude d'un procédé hybride Adsorption / Bioréacteur à membranes pour le traitement des effluents industriels. PhD Thesis

Li C, Moe WM (2005) Activated carbon load equalization of discontinuously generated acetone and toluene mixtures treated by biofiltration. Environ Sci Technol 39:2349–2356

Mason CA, Ward G, Abu-Salah K et al (2000) Biodegradation of BTEX by bacteria on powdered activated carbon. Bioprocess Eng 23:331–336

Merle T (2009) Couplage des procédés d'adsorption et d'ozonation pour l'élimination de molécules bio-récalcitrantes. PhD thesis, University of Toulouse

Moe WM, Li C (2005) A design methodology for activated carbon load equalization systems applied to biofilters treating intermittent toluene loading. Chem Eng J 113:175–185

Muhammad Khan MA, Choong TSY et al (2011) Desorption of β-carotene from mesoporous carbon coated monolith: isotherm, kinetics and regeneration studies. Chem Eng J 173:474–479

Nabatilan MM, Moe WM (2010) Effects of water vapor on activated carbon load equalization of gas phase toluene. Water Res 44:3924–3934. doi:10.1016/j.watres.2010.04.028

Ottengraf SPP (1986) Exhaust gas purification. In: Rehm HJ, Reed G (eds) VCH Verlagsgesellschaf, vol 8. Weinheim, Germany, p 426

Ozkaya B (2006) Adsorption and desorption of phenol on activated carbon and a comparison of isotherm models. J Hazard Mater 129:158–163. doi:10.1016/j.jhazmat.2005.08.025

Perry RH, Chilton CH (1973) Chemical engineers' handbook, 5th edn. McGraw-Hill, New York

Ruthven DM (1984) Principles of adsorption and adsorption processes. Wiley, New York

Sing KSW (1985) Reporting physisorption data for gas/solid systems with special reference to the determination of surface area and porosity (Recommendations 1984)

Snoeyink VL, Weber WJ, Mark HB (1969) Sorption of phenol and nitrophenol by active carbon. Environ Sci Technol 3:918–926

Tanthapanichakoon W, Ariyadejwanich P, Japthong P et al (2005) Adsorption–desorption characteristics of phenol and reactive dyes from aqueous solution on mesoporous activated carbon prepared from waste tires. Water Res 39:1347–1353. doi:10.1016/j.watres.2004.12.044

Tchobanoglous G, Burton FL, Stensel HD (2002) Wastewater engineering: treatment and reuse, 4th edn. McGraw-Hill Science/Engineering/Math, Boston

Tien C (1995) Adsorption calculations and modeling. Butterworth-Heinemann, Boston

Wakao N, Funazkri T (1978) Effect of fluid dispersion coefficients on particle-to-fluid mass transfer coefficients in packed beds: Correlation of sherwood numbers. Chem Eng Sci 33:1375–1384

Wani AH, Branion RMR, Lau AK (1998) Effects of periods of starvation and fluctuating hydrogen sulfide concentration on biofilter dynamics and performance. J Hazard Mater 60:287–303

Weber FJ, Hartmans S (1995) Use of activated carbon as a buffer in biofiltration of waste gases with fluctuating concentrations of toluene. Appl Microbiol Biotechnol 43:365–369